Dynamics of Solar and Stellar Convection Zones and Atmospheres
Proceedings IAU Symposium No. 365, 2024
A. V. Getling & L. L. Kitchatinov, eds.
doi:10.1017/S1743921324000413

Probing the superadiabaticity of the solar convection zone with inertial modes

Prithwitosh Dey[1], **Yuto Bekki**[1], **and Laurent Gizon**[1,2]

[1]Max–Planck-Institut für Sonnensystemforschung, 37077 Göttingen, Germany
email: dey@mps.mpg.de

[2]Institut für Astrophysik, Georg–August-Universität Göttingen, 37077 Göttingen, Germany

Abstract. Our understanding of solar convection is incomplete. A crucial gap is the unknown superadiabaticity in the solar convection zone, $\delta = \nabla - \nabla_{\rm ad}$. Global modes of oscillations in the inertial frequency range are sensitive to δ and serve as a novel tool to explore solar convection. Here, we address the forward problem where the superadiabaticity $\delta(r)$ varies with radius. We solve the 2.5D eigenvalue problem, considering the linearized equations for momentum, mass and energy conservation with respect to a realistic solar model. We find that the frequency and eigenfunction of the $m = 1$ high-latitude mode are influenced by δ in the lower convection zone. Our prescribed setup suggests that the superadiabaticity in the lower half of the convection zone is below 2.4×10^{-7} to reach a qualitative agreement with the observed eigenfunction.

Keywords. Sun: interior, Sun: oscillations, Sun: helioseismology, Sun: convection

1. Introduction

In the outer 30% of the Sun's interior, the thermal energy is transported by convection. Since convection can efficiently mix the entropy, the mean stratification in the convection zone (CZ) is believed to be very close to adiabatic. A tiny deviation from the adiabatic stratification is measured by the superadiabaticity

$$\delta = \nabla - \nabla_{\rm ad} = -\frac{H_{\rm p}}{c_{\rm p}} \frac{ds_0}{dr},$$

where $\nabla = d \ln T / d \ln p$ is the double-logarithmic temperature gradient, $H_{\rm p}$ is the pressure scale height, $c_{\rm p}$ is the specific heat at constant pressure, and s_0 denotes the horizontal mean of the background entropy. The stratification is convectively unstable when $\delta > 0$ (superadiabatic) and is convectively stable when $\delta < 0$ (subadiabatic). According to the local mixing-length model (Böhm-Vitense 1958), δ is estimated to be of the order of 10^{-6}. Acoustic modes, which are the subject of conventional p-mode helioseismology are largely insensitive to the value of δ.

Evidence indicates that the solar convection cannot be described by local mixing-length models. Time-distance helioseismology has provided an observational upper limit on the subsurface convective velocity at large scales which are much smaller than the typical convective speed estimated by the mixing-length model (Hanasoge et al. 2012). Furthermore, recent numerical simulations (which are consistent with the local mixing-length model) have difficulty in reproducing the observed differential rotation of the Sun (e.g., Hotta et al. 2023). These problems are referred to as the convective conundrum (O'Mara et al. 2016). It has been implied that the solar convective energy transport is a highly non-local process (Brandenburg 2016) and the mean stratification in the CZ could be much less superadiabatic than typically assumed (Cossette and Rast 2016).

Recent numerical simulations also show that a weakly subadiabatic layer can exist near the bottom of the CZ as a result of non-local convective heat transport (Hotta et al. 2022; Käpylä 2023).

Recently, various kinds of inertial modes have been detected and identified on the Sun. They are global-scale low-frequency modes of oscillation restored by Coriolis force. The observed solar inertial modes include the equatorial Rossby modes (Löptien et al. 2018; Liang et al. 2019; Proxauf et al. 2020; Mandal and Hanasoge 2020), high-latitude and mid-latitude modes (Gizon et al. 2021) and others (Hanson et al. 2022). Theoretical models of the solar inertial modes predict that some modes are highly sensitive to the superadiabaticity δ in the CZ (Bekki et al. 2022; Bekki 2024). It was demonstrated through numerical studies by Gizon et al. (2021) that the mode structure can be reproduced with $\delta \leq 2 \times 10^{-7}$. However, these studies have used the simplifying assumption of a spatially constant δ. Here, we go a step further and aim to constrain the superadiabaticity in the CZ as a function of radius $\delta(r)$ by solving the forward problem of the solar inertial modes.

2. The forward problem

The model equations consist of the linearized equations of motion, continuity, and energy conservation, in a frame rotating at the Carrington angular velocity Ω_0. The magnetic field is not included. We consider a realistic solar background stratification (Christensen–Dalsgaard et al. 1996), the differential rotation measured by global helioseismology (Larson and Schou 2018), and the latitudinal entropy gradient required to sustain the observed differential rotation via thermal wind balance. For simplicity, uniform viscous and thermal diffusivities of 5×10^{11} cm^2 s^{-1} are chosen.

The function $\delta(r)$ enters the linearised energy equation:

$$\frac{Ds_1}{Dt} = c_\mathrm{p}\delta\frac{v_r}{H_\mathrm{p}} - \frac{v_\theta}{r}\frac{\partial s_0}{\partial\theta} + \frac{1}{\rho_0 T_0}\nabla\cdot(\kappa\rho_0 T_0\nabla s_1), \tag{1}$$

where the variables have their usual meaning, the subscript 0 is for the background values, and the subscript 1 is for the wave perturbations (Gizon et al. 2021, their appendix B.1). The quantities v_r and v_θ are the radial and colatitudinal components of wave velocity. Furthermore, we parameterize the function $\delta(r)$ as follows:

$$\delta(r) = \delta_\mathrm{lower} + \left(\frac{\delta_\mathrm{upper} - \delta_\mathrm{lower}}{2}\right)\left[1 + \tanh\left(\frac{r - r_\mathrm{mid}}{d}\right)\right], \tag{2}$$

where δ_upper and δ_lower denote the superadiabaticity in the upper and lower CZ, respectively. The transition from δ_lower to δ_upper occurs at $r = r_\mathrm{mid}$ with a transition width d. In this study, we fix $d = 0.03R_\odot$ and δ_lower, δ_upper, r_mid are parameters to be varied.

We use the linear eigenvalue solver of the differentially-rotating CZ from Bekki et al. (2022). It is a 2.5D solver, which computes the eigenmodes of oscillation in the inertial frequency range at fixed longitudinal wavenumber m, over a staggered grid in radius and colatitude. The radial domain is $0.710 \leq r/R_\odot \leq 0.985$.

3. Outlook

Our preliminary results concern the high-latitude mode with $m = 1$ and the equatorial Rossby mode with $m = 3$. The real part of the eigenfrequency, ω^sim, and the horizontal velocity eigenfunction at the surface, $\mathbf{v}^\mathrm{sim}(\theta, \phi)$, are computed for various combinations of $(\delta_\mathrm{lower}, \delta_\mathrm{upper}, r_\mathrm{mid})$. The function $\delta(r)$ can then be constrained using the observations ω^obs and $\mathbf{v}^\mathrm{obs}(\theta, \phi)$ reported by Gizon et al. (2021, their table A1).

We find that the surface eigenfunction of the $m = 1$ high-latitude mode is strikingly sensitive to the value of the superadiabaticity in the lower half of the CZ, δ_lower. Figure 1

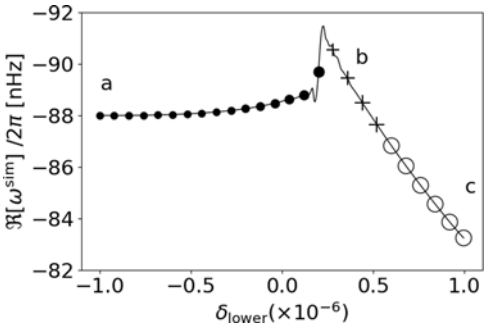

Figure 1. Variation of the frequency of the $m = 1$ high-latitude mode as a function of $\delta_{\rm lower}$. Filled circles mark the modes whose eigenfunctions have the same direction of spiralling as the observations (cf. Fig. 2a), plus symbols mark the modes with no distinct spiralling (cf. Fig. 2b), and open circles show modes with reverse spiralling (cf. Fig. 2c). The size of the marker is proportional to the (positive) growth rate of the modes. The value of $\delta_{\rm lower}$ covers the range $\pm 10^{-6}$, while the parameters $\delta_{\rm upper} = 0$ and $r_{\rm mid} = 0.85 R_\odot$ are fixed.

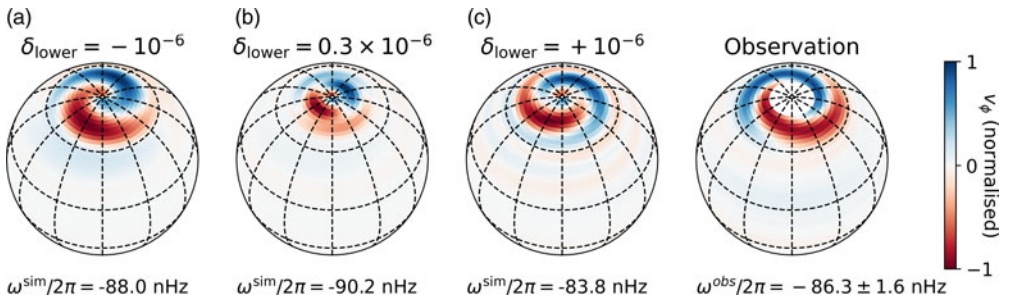

Figure 2. Longitudinal component of the velocity eigenfunction of the $m = 1$ high-latitude mode, indicated by different symbols in Fig. 1. Left to right: mode with the correct spiralling, marked with filled circles; mode with indistinct spiralling, marked with plus symbols; mode with reverse spiralling, marked with open circles; observation. The observation shown uses data from the HMI ring diagram pipeline with 5° tiles (Gizon et al. 2021).

illustrates how the frequency and the inclination of the spiral pattern of the v_ϕ eigenfunction depends on $\delta_{\rm lower}$, for fixed $\delta_{\rm upper} = 0$ and $r_{\rm mid} = 0.85 R_\odot$. We find that the direction of spiralling matches the observation for $\delta_{\rm lower} < 2.4 \times 10^{-7}$, and reverses sign for $\delta_{\rm lower} > 5.5 \times 10^{-7}$. For $\delta_{\rm lower}$ between these values, the direction of spiral is unclear. Sample eigenfunctions for all three cases are shown in Fig. 2. For this particular set-up, we can therefore conclude that in order to recreate the observed latitudinal profile of the mode, the superadiabaticity in the lower half of the convection zone must be less than 2.4×10^{-7}.

Unlike the $m = 1$ high-latitude mode, we find that the $m = 3$ equatorial Rossby mode with zero radial node is rather insensitive to changes in $\delta_{\rm lower}$, as shown in Fig. 3, likely due to their toroidal nature. In future work, we will carry out a comprehensive study of the sensitivity of selected inertial modes to more general radial profiles of $\delta(r)$ and of the turbulent viscosity profile $\nu_{\rm turb}(r)$.

Acknowledgements

We acknowledge support from ERC Synergy Grant WHOLESUN 810218 and Deutsche Forschungsgemeinschaft (DFG, German Research Foundation) through SFB 1456/432680300 Mathematics of Experiment, project C04. P.D. acknowledges support

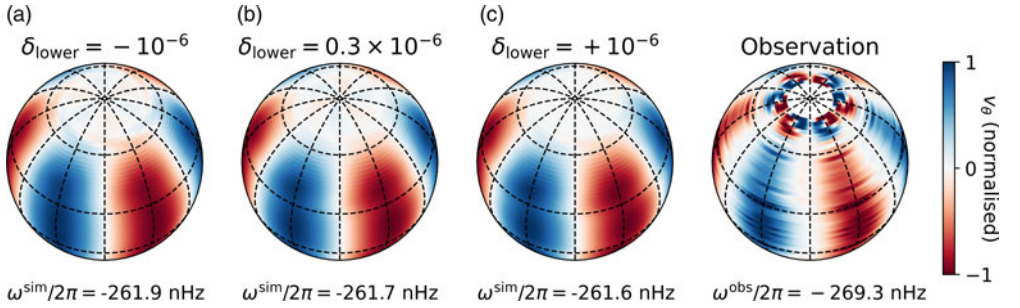

Figure 3. Colatitudinal component of the velocity eigenfunction of the $m = 3$ Rossby mode.

from the International Max–Planck Research School (IMPRS) for Solar System Science at the University of Göttingen. The HMI data are courtesy of NASA/SDO and the HMI Science Team.

References

Bekki, Y. 2024, Numerical study of non-toroidal inertial modes with $l = m + 1$ radial vorticity in the Sun's convection zone. *Astron. Astrophys.*, 682, A39.

Bekki, Y., Cameron, R. H., & Gizon, L. 2022, Theory of solar oscillations in the inertial frequency range: Linear modes of the convection zone. *Astron. Astrophys.*, 662, A16.

Bogart, Richard S. and Baldner, Charles S. and Basu, Sarbani 2015, Evolution of Near-surface Flows Inferred from High-resolution Ring-diagram Analysis. *Astrophys. J.*, 807, 125.

Böhm-Vitense, E. 1958, Über die Wasserstoffkonvektionszone in Sternen verschiedener Effektivtemperaturen und Leuchtkräfte. *Zeitschrift Astrophys.*, 46, 108.

Brandenburg, A. 2016, Stellar Mixing Length Theory with Entropy Rain. *Astrophys. J.*, 832, 6.

Christensen–Dalsgaard, J., Dappen, W., Ajukov, S. V., Anderson, E. R., Antia, H. M., Basu, S., Baturin, V. A., Berthomieu, G., Chaboyer, B., Chitre, S. M., Cox, A. N., Demarque, P., Donatowicz, J., Dziembowski, W. A., Gabriel, M., Gough, D. O., Guenther, D. B., Guzik, J. A., Harvey, J. W., Hill, F., Houdek, G., Iglesias, C. A., Kosovichev, A. G., Leibacher, J. W., Morel, P., Proffitt, C. R., Provost, J., Reiter, J., Rhodes, Jr., E. J., Rogers, F. J., Roxburgh, I. W., Thompson, M. J., & Ulrich, R. K. 1996, The Current State of Solar Modeling. *Science*, 272, 1286–1292.

Cossette, J.-F. & Rast, M. P. 2016, Supergranulation as the Largest Buoyantly Driven Convective Scale of the Sun. *Astrophys. J.*, 829, L17.

Gizon, L., Cameron, R. H., Bekki, Y., Birch, A. C., Bogart, R. S., Sacha Brun, A., Damiani, C., Fournier, D., Hyest, L., Jain, K., Lekshmi, B., Liang, Z.-C., & Proxauf, B. 2021, Solar inertial modes: Observations, identification, and diagnostic promise. *Astron. Astrophys.*, 652, L6.

Hanasoge, S. M., Duvall, T. L., & Sreenivasan, K. R. 2012, Anomalously weak solar convection. *PNAS*, 109, 11928–11932.

Hanson, C. S., Hanasoge, S., & Sreenivasan, K. R. 2022, Discovery of high-frequency retrograde vorticity waves in the Sun. *Nat. Astron.*, 6, 708–714.

Hotta, H., Bekki, Y., Gizon, L., Noraz, Q., & Rast, M. 2023, Dynamics of Large-Scale Solar Flows. *Space Sci. Rev.*, 219, 77.

Hotta, H., Kusano, K., & Shimada, R. 2022, Generation of Solar-like Differential Rotation. *Astrophys. J.*, 933, 199.

Käpylä, P. J. 2023, Convective scale and subadiabatic layers in simulations of rotating compressible convection. Preprint, https://arxiv.org/abs/2310.12855.

Larson, T. P. & Schou, J. 2018, Global-Mode Analysis of Full-Disk Data from the Michelson Doppler Imager and the Helioseismic and Magnetic Imager. *Sol. Phys.*, 293, 29.

Liang, Z.-C., Gizon, L., Birch, A. C., & Duvall, T. L. Jr. 2019, Time-distance helioseismology of solar Rossby waves. *Astron. Astrophys.*, 626, A3.

Löptien, B., Gizon, L., Birch, A. C., Schou, J., Proxauf, B., Duvall, T. L., Bogart, R. S., & Christensen, U. R. 2018, Global-scale equatorial Rossby waves as an essential component of solar internal dynamics. *Nat. Astron.*, 2, 568–573.

Mandal, K. & Hanasoge, S. 2020, Properties of Solar Rossby Waves from Normal Mode Coupling and Characterizing Its Systematics. *Astrophys. J.*, 891, 125.

O'Mara, B., Miesch, M. S., Featherstone, N. A., & Augustson, K. C. 2016, Velocity amplitudes in global convection simulations: The role of the Prandtl number and near-surface driving. *Adv. Space Res.*, 58, 1475–1489.

Proxauf, B., Gizon, L., Löptien, B., Schou, J., Birch, A. C., & Bogart, R. S. 2020, Exploring the latitude and depth dependence of solar Rossby waves using ring-diagram analysis. *Astron. Astrophys.*, 634, A44.